E-ISSN: 2829-7687
Journal of Fibers and Polymer Composites
Vol. 4 No. 2 (025): 101-120

Enhancement of Aluminium-Air Battery Performance Using Rice Husk-Derived Carbon Quantum Dots and Carbon Nanotubes

Muhammad Ammar Zakky [a], Firman Ridwan [a *], Dean Bilalwa Agusto [a], Wismalqi [a], Gusriwandi [a]

[a] Department of Mechanical Engineering, Universitas Andalas, Padang, Indonesia

Abstract. *The advancement of sustainable and efficient energy storage systems is vital for tackling the challenges posed by the integration of renewable energy sources and the constraints of conventional lithium-ion batteries. This research explored the potential of an innovative electrolyte membrane for aluminium-air batteries, which incorporates carbon quantum dots (CQDs) sourced from rice husk charcoal and carbon nanotubes (CNTs) within a polyvinyl alcohol (PVA) framework. CQDs were synthesized using a microwave-assisted technique, and CNTs were added to enhance the structural and conductive properties of the membranes. Three distinct membrane compositions were prepared: a base solution of PVA, HCl, and glycerol; a base solution with CQDs; and a base solution with CQDs and CNTs. Fourier Transform-Infrared (FT-IR) spectroscopy revealed enhanced intermolecular interactions and successful integration of the carbon nanomaterials within the polymer network. X-ray diffraction (XRD) analysis indicated a reduction in crystallite size from 11.27 nm (base membrane) to 9.65 nm (–14.36%) with CQDs and further to 8.29 nm (–26.47%) with CQDs + CNTs, suggesting improved amorphous characteristics that reinforce the membrane structure and facilitate ionic conductivity. Electrochemical impedance spectroscopy (EIS) demonstrated an increase in ionic conductivity from 4.98501 mS/cm (base membrane) to 5.51837 mS/cm with CQDs and 6.35292 mS/cm (+27.4%) with CQDs + CNTs. These findings highlight the synergistic effect of CQDs and CNTs in optimizing the ion migration pathways and charge transport within the electrolyte membrane. The utilization of rice husk charcoal as a precursor for CQDs aligns with sustainable practices and promotes the use of renewable resources. This research introduces an innovative method for creating advanced electrolyte membranes for aluminium-air batteries, playing a role in creating energy storage solutions that are efficient, eco-friendly, and economical.*

Keywords: *Aluminium-Air Battery; Carbon Quantum Dots; Carbon Nanotubes; Nanocomposite Membrane; Ion Conductivity.*

Type of the Paper: Regular Article.

1. Introduction

Dependence on a limited number of energy sources can render a nation's energy infrastructure susceptible to global price volatility, geopolitical tensions, or supply interruptions [1]. The integration of renewable energy sources contributes to a more diversified and resilient energy portfolio. This issue underscores the importance of adopting renewable energy sources such as solar and wind, which, despite their potential, face challenges related to supply continuity due to their dependence on natural conditions [2]. To address fluctuations in renewable energy

https://doi.org/10.55043/jfpc.v4i2.403
Received July 31, 2025; Received in revised form September 6, 2025; Accepted October 6, 2025; Published October 31, 2025

* First corresponding author;
Email: firmanridwan@eng.unand.ac.id

supply, energy storage systems, particularly batteries, are essential. Battery technology facilitates stable and efficient energy distribution, especially in portable devices, electric vehicles, and integrated energy systems [3].

Lithium-ion batteries, while extensively utilized [4], are beginning to face notable constraints. The environmental ramifications associated with heavy metal usage, coupled with safety issues such as fire risks and limited energy capacity, make these batteries less than ideal for sustainable long-term application [5]. To address these challenges, researchers are exploring various alternative battery technologies. Among these, the aluminium-air battery emerges as a promising option [5]. This technological advancement utilizes aluminium as the anode while simultaneously extracting oxygen from the ambient atmosphere to serve as the cathode, facilitating energy production through a redox reaction in an open system [6]. Aluminium presents several benefits, including its natural abundance, superior safety profile compared to lithium, and a significantly higher theoretical energy density [7].

The efficacy of an aluminium-air battery is predominantly determined by its electrolyte components, with the electrolyte membrane playing a pivotal role [8]. This membrane acts as an ion conduction medium and a separator between electrodes [9]. Enhancing ionic conductivity and membrane stability can be achieved through the integration of functional nanomaterials. Carbon Quantum Dots (CQDs), derived from rice husk charcoal, possess notable attributes such as nanoscale particle size, amorphous structure, and high hydrophilicity [10], in partnership with functional entities such as hydroxyl and carboxyl groups [11]. These features enhance electrolyte interaction, extend ionic pathways, and improve the thermal and chemical stability of the membrane [10]. Utilizing rice husk charcoal as a source for Carbon Quantum Dots (CQDs) not only offers ecological advantages by converting agricultural waste into advanced functional materials but also aligns with green chemistry principles by employing renewable resources and reducing environmental impact [12].

To enhance the structural integrity and conductive pathways within the membrane, Carbon Nanotubes (CNTs) are incorporated as a reinforcing agent [13]. CNTs possess a cylindrical configuration characterized by high mechanical strength and exceptional electrical conductivity, rendering them ideal for establishing ion-mediated networks and augmenting the overall performance of electrolyte membranes [14]. The amalgamation of carbon quantum dots (CQDs) obtained from rice husk with carbon nanotubes (CNTs) within a polymeric matrix is anticipated to yield a porous nanocomposite membrane that facilitates efficient ion delivery and ensures long-term operational stability [15]. This innovation represents a significant advancement in the development of a new generation of aluminium-air battery systems that are more reliable, environmentally sustainable, and cost-effective, thereby contributing to national energy security

[16]. CQDs have also been integrated into nanofiber structures used in battery components, offering additional benefits beyond their application in polymer membranes. Nanofibers have a high surface area and porous morphology that can facilitate ion transport, stabilize electrolytes, and enhance adhesion to electrodes [17]. Previous studies demonstrating improved porosity, electrolyte uptake, and safety compared with conventional separators [18]. Therefore, the development of CQD-loaded nanofiber membranes is expected to further optimize the ionic conductivity while contributing to the structural reinforcement of aluminium-air batteries.

Various studies have investigated carbon- and silica-based materials sourced from biomass to enhance battery performance. In 2019, Liu *et al.* [19] designed a hybrid architecture based on MoS_2@graphene interpenetrated by carbon nanofibers, resulting in a conductive structure that enhances the mechanical stability and long-term performance of sodium-ion batteries, achieving a high specific capacity of 598 mAh/g and stability over 1000 cycles. In the same year, Zheng *et al.* [20] reviewed the application of various configurations of carbon nanotubes (CNTs) in lithium-sulfur batteries, highlighting the advantages of the one-dimensional structure of CNTs in forming a conductive network and mitigating the polysulfide shuttle effect. Razzaq *et al.* [21] also developed a sulfur- and CNT-based binder-free film electrode via electrospinning, achieving an initial capacity of 1610 mAh/g and high cycle stability up to 500 cycles at 1C, attributed to the synergistic effect of CNTs and the material's porosity. Research by Palanisamy *et al.* [22] demonstrated the potential of palm shell-modified nano-activated carbon as a cathode in aluminium metal–oxygen batteries, where the material's microstructure and high surface area enhanced electrochemical performance with PVA-based gel electrodes.

In 2020, Yang *et al.* [23] conducted an evaluation of the dithiothreitol (DTT) additive within an aluminium–air battery alkaline electrolyte system, achieving notable improvements in the stability of the aluminium anode and the efficiency of redox reaction reversibility. In a separate study, Mori *et al.* [24] provided a comprehensive review of advancements in Al–air battery technology, underscoring the challenges associated with anode degradation and the necessity for cost-effective electrocatalysts for the cathode. The review also highlighted the potential of biomass-based carbon as a viable alternative to conventional catalysts. Hu *et al.* [25] explored lithium–sulfur batteries as a promising substitute for lithium-ion batteries in high-capacity energy storage applications. The primary challenge in this technology is the protection of the lithium anode, particularly under conditions of high sulfur loading. To address this, the study introduced the incorporation of graphene quantum dots (GQDs) in the electrolyte as a strategy to suppress dendrite growth. This modification of the anolyte successfully enhanced the critical current and cycling stability, presenting a novel approach to improving lithium anode performance. Zhu *et al.* [26] asserted that carbon quantum dots (CQDs) possess significant potential in energy storage applications due to their unique properties. However, challenges persist regarding low synthesis yield and electrical conductivity. Through a large-scale synthesis approach, the study achieved a graphitic CQDs yield exceeding 50%, markedly enhancing electrochemical performance. The developed NS-CQDs/$NiCo_2S_4$ composite exhibited superior performance in aqueous-based batteries, underscoring the critical role of CQDs in the future of battery technology.

Zhou *et al.* [27] introduced an innovative sulfur-containing material characterized by a flower-shaped $Bi_4Ti_3O_{12}$ architecture, synergistically combined with carbon nanotubes (BTO/CNT), is proposed for utilization in lithium-sulfur battery systems. The ferroelectric properties of $Bi_4Ti_3O_{12}$ induce spontaneous polarization, facilitating polysulfide conversion and mitigating the shuttle effect through robust Lewis's acid-base interactions. The carbon nanotubes establish a conductive network that enhances electron transport. This composite material demonstrates high cycle stability, with a capacity degradation rate of merely 0.037% per cycle over 1000 cycles, indicating its potential as an advanced material for high-performance lithium–sulfur batteries. In 2022, Sun *et al.* [28] employed rice husk to synthesize SiOx particles, which were subsequently encapsulated within a graphene aerogel. This hybrid structure exhibited a high capacity of 1327 mAh/g and maintained good cycling stability after 200 cycles, attributed to enhanced ionic and electronic conductivity provided by the conductive aerogel and nanoscale pore structure. Concurrently, Xiaofei *et al.* [29] assessed activated carbon derived from rice husk as an additive for lead-carbon batteries, finding that the specific surface area, ash content, and pore structure significantly influenced the capacity efficiency and conductivity of the electrode. Kumar *et al.* [30] investigated the potential of Carbon Quantum Dots (CQDs) as a liquid electrolyte for graphene-based supercapacitors. The application of a 25 mM CQDs solution yielded a gravimetric capacitance of 155 F/g at a current density of 1 A/g and an energy density of approximately 55 Wh/kg. This study also introduced a flexible electrolyte film based on polymer gel–CQDs (f-CPG), which exhibited high ionic conductivity (0.48 S/cm) and excellent electrochemical performance, reinforcing the viability of CQDs as a promising alternative in energy storage systems.

Liu *et al.* [31] presented a LiCl salt-based PVA electrolyte designed for flexible aluminium–air batteries, achieving a conductivity of 4.3 mS/cm, which is comparable to that of solutions. This innovation supports high flexibility and stable performance even when the battery is bent or folded. In a separate study, Luo *et al.* [32] engineered a CQDs/NiCo-LDHs electrode in the form of nanosheets for use in flexible supercapacitors. This electrode demonstrated a specific capacitance of 2023 F/g, with an energy density of 117.8 Wh/kg and a power density of 528.3 W/kg, underscoring the significant potential of CQDs in the development of high-performance electrodes for flexible energy storage devices. Meanwhile, Lu *et al.* [33] addressed the challenges faced by hybrid supercapacitors (HSCs), particularly the kinetic imbalance between the cathode and anode that restricts energy density. To mitigate this issue, they developed a cathode material composed of an N-doped CQDs/Ni–Co–Se composite through a hydrothermal process. This material exhibited enhanced ion and electron transfer rates, attaining an energy density of 23.1 Wh/kg while simultaneously achieving a power density of 38.3 kW/kg. These findings propose a novel approach for the development of high-rate battery-type electrode materials.

Wang *et al.* [34] developed hollow bimetallic cage nanostructures (Ni–Fe–S/NCQDs) enhanced with nitrogen-doped carbon quantum dots for use in zinc–air batteries. This composite demonstrated a half-wave potential of 0.85 V during the oxygen reduction reaction (ORR) and a minimal overpotential of 0.295 V for the oxygen evolution reaction (OER). The open hollow design facilitated improved mass transfer and exposure of active sites, maintaining high stability after numerous cycles, thus presenting a novel approach to boosting ORR/OER electrocatalytic performance. Shaker *et al.* [35] recently reviewed cutting-edge electrode materials for secondary ion batteries, emphasizing carbon dots (CDs) and graphene quantum dots (GQDs). Whether used alone or in composites, these materials have been proven to enhance the capacity and electrochemical characteristics of various battery types, such as lithium-ion and sodium-ion. The study concludes with a prospective outlook on CQD research in high-energy battery systems.

Pallavolu *et al.* [36] devised an innovative approach to synthesize carbon quantum dots (CQDs) utilizing lemon juice, underscoring the method's environmental friendliness for supercapacitor applications. The incorporation of heteroatoms, specifically nitrogen (N) and sulfur (S), into the CQDs significantly enhanced their electrochemical performance by improving ion and electron mobility. The specific capacities were measured at 284 mAh/g for undoped CQDs, 181 mAh/g for N-doped CQDs, and 125 mAh/g for S-doped CQDs. Notably, S-doped CQDs maintained 94.5% of their capacitance over 10,000 cycles, with a Coulombic efficiency of 98%. The resulting symmetric supercapacitor exhibited a specific capacity of 21.7 mAh/g and an energy density of 15.2 Wh/kg. In a pertinent investigation, Patwari *et al.* [37] examined the efficacy of a composite material comprising activated carbon and rice husk ash functioning as a cathode catalyst in aluminium–air batteries. This study demonstrated a voltage increase of up to 20% and showed promising stability, suggesting that recycled materials could effectively reduce production costs and lessen environmental impact.

Numerous strategies have been devised to enhance ionic conductivity and battery capacity, primarily through the modification of electrolyte materials and the incorporation of conductive additives. Rice husk charcoal presents a promising precursor for the synthesis of carbon quantum dots (CQDs), which are nanoparticles characterized by exceptional electrical and optical properties. This method converts rice husk waste into a valuable material for energy technology, while simultaneously encouraging the utilization of renewable resources and reducing reliance on synthetic materials or heavy metals [38]. Consequently, rice husk charcoal-derived CQDs hold significant potential for application in aluminium-air batteries. Although CQDs are frequently employed in sensors and optoelectronic devices, their use in PVA/HCl/glycerol-based electrolyte membranes for aluminium-air batteries remains largely unexplored.

This study focuses on the enhancement of ionic conductivity, membrane physical properties, and the overall performance of aluminium-air batteries. The integration of carbon quantum dots (CQDs) and carbon nanotubes (CNTs) fortifies the intermolecular bonds within the electrolyte structure, leading to improved conductivity and system performance. In light of the potential of CQDs in sulfur oxide batteries, this research synthesizes CQDs from rice husk charcoal and integrates them with CNTs. The convergence of battery technology and waste management expands the possibilities for innovation in sustainable energy systems. Employing locally sourced carbon nanomaterials presents a cost-effective and environmentally sustainable solution, promoting energy efficiency and resource conservation.

2. Materials and Methods

2.1. Materials

This study employed Carbon Quantum Dots (CQDs) as the primary matrix for membrane fabrication. Rice husk charcoal was utilized as a starting material to produce the CQDs, utilizing a Microwave-Assisted technique. The rice husks employed in this study were sourced from Limau Manis, Pauh, Padang City, West Sumatra, Indonesia. Prior to use, the rice husks were meticulously cleaned with distilled water to eliminate dust and contaminants, and then left to dry in natural conditions. The dried husk underwent a carbonization process in a furnace set at 400 °C for a duration of 2 h, resulting in the formation of rice husk charcoal. After naturally cooling to room temperature inside the furnace, the rice husk charcoal was pulverized into a fine powder and kept in airtight containers for the later production of carbon quantum dots (CQDs).

Carbon Nanotubes (CNTs) were incorporated using MWCNT C2001. Polyvinyl Alcohol (PVA, MW ~60,000), procured from Merck, was employed as a supplementary polymer to augment the physical characteristics of the membrane. Hydrochloric Acid (HCl) was incorporated into the matrix to boost ionic conductivity. Glycerol, also sourced from Merck, functioned as a thickening agent within the electrolyte membrane. Citric Acid ($C_6H_8O_7$), sourced from Merck, was utilized for both oxidation and functionalization in the production of CQDs. The nanofiber, serving as a composite material, was produced from Polylactic Acid (PLA, MW ~60,000) using Dimethylformamide and Acetone as solvents, via the electrospinning method. In order to guarantee uniformity and reliability, the integrity and purity of all elements employed in this research were rigorously ascertained.

2.2. Preparation of Carbon Quantum Dots

As illustrated in Fig. 1, the creation of CQDs sourced from rice husk charcoal involves microwave-assisted treatment of the precursor to obtain a CQD solution. Three g of rice husk charcoal were precisely measured. Initially, a volume of 10 mL of distilled water was introduced into a beaker and subjected to heating while concurrently being agitated utilizing a magnetic stirrer. Next, a quantity of 3 g of Citric Acid ($C_6H_8O_7$) was introduced into the beaker and stirred until they completely dissolved. The rice husk charcoal was then introduced into the mixture and stirred for 10 min at a speed of 125 rpm. Subsequent to the agitation procedure, the resultant solution was subjected to microwave irradiation for a duration of three min to facilitate

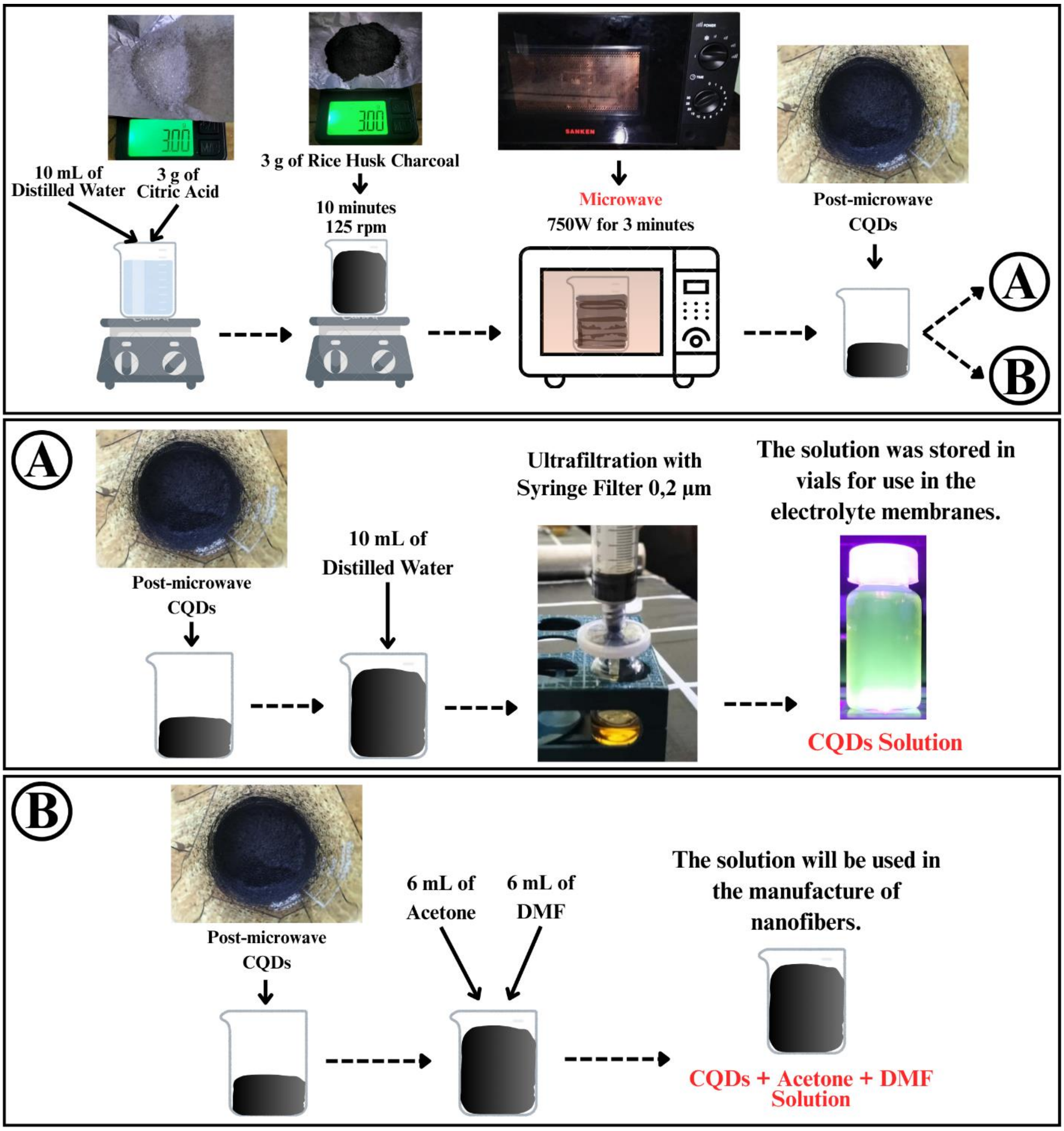

Fig. 1. CQDs Fabrication Process for The Electrolyte Membranes and Nanofiber.

the acceleration of the synthesis process. This procedure was conducted on two separate occasions for distinct objectives. Initially, following the microwave treatment, 20 mL of distilled water was added to the beaker, and the resultant mixture was stirred comprehensively prior to being subjected to a 0.22 µm pore syringe filter to remove larger particulates and contaminants. The resultant filtrate, which comprised pure Carbon Quantum Dots (CQDs), was subsequently preserved in a vial for future application in the development of the electrolyte membrane. In the second stage, following microwave heating, the reaction solution was further processed by adding a mixture of organic solvents, comprising 6 mL of acetone and 6 mL of dimethylformamide (DMF), into a test tube containing CQDs. This mixture was utilized to produce a CQDs solution that was more compatible for integration with the polymer solution in the fabrication of nanofibers [39].

To avoid ambiguity, it should be noted that CQDs were incorporated through two distinct procedures depending on the host polymer. CQDs were dispersed in water for the preparation of PVA-based membranes because of the hydrophilic and water-soluble nature of PVA [40]. Meanwhile, in the preparation of PLA-based nanofibers, CQDs were incorporated into the polymer solution dissolved in DMF because PLA is not water-soluble and requires an organic solvent [41]. This difference in approach ensured the proper dispersion of CQDs in both polymer matrices.

2.3. Nanofiber Preparation

As shown in Fig. 2, the preparation of nanofiber membranes via electrospinning involves dissolving PLA in acetone/DMF, incorporating rice husk-derived CQDs into the polymer solution, and producing nanofiber mats through the electrospinning process. In addition to membrane casting, CQDs were incorporated into nanofiber structures to exploit the inherent benefits of nanofiber-based electrolytes. Nanofibers exhibit interconnected porosity and a large surface area, which promote effective ion transport and improve electrolyte uptake [18]. Furthermore, electrospun nanofibers enhance the structural integrity and thermal stability of the separator membrane, offering greater safety than conventional membranes [17]. These features justify the preparation of CQDs/PLA nanofibers through electrospinning.

The polymer solution was prepared by dissolving 2 g of polylactic acid (PLA) into 6 mL of acetone within a 50 mL beaker. The mixture was then stirred with a magnetic stirrer for 10 min at 60°C until the PLA was fully dissolved. Afterward, 6 mL of dimethylformamide (DMF) was added to the solution, and stirring continued for another 10 min at room temperature to ensure a uniform solvent mixture. Thereafter, 5 mL of Carbon Quantum Dots (CQDs) solution was incorporated into the mixture, which was then stirred for another 10 min at 60°C to ensure uniform dispersion of the CQDs within the polymer solution. The resultant solution was subsequently employed in the nanofiber formation process utilizing the electrospinning technique. This electrospinning unit consisted of necessary elements like a power supply, a syringe, a brushed DC motor, and a collector. The nanofiber fabrication process maintained a consistent feed rate of 0.3 mL/min, with a high-voltage supply set to 20 kV (10 mA). A syringe with a diameter of 38 mm (18G x 1½") was employed for this procedure [42].

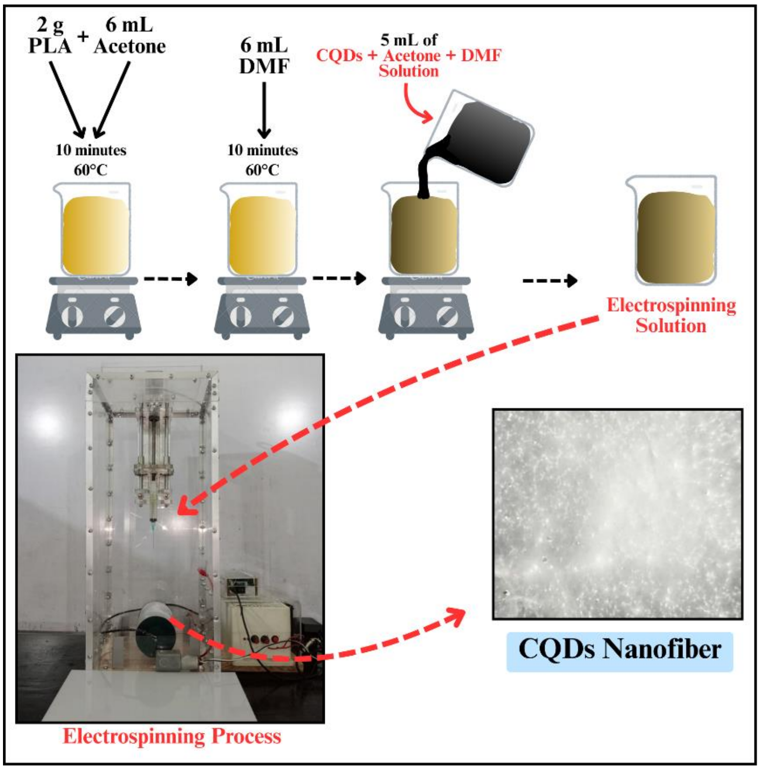

Fig. 2. CQDs Nanofiber Manufacturing Process Using The Electrospinning Method.

2.4. Electrolyte Membrane Preparation

The fabrication steps of the gel electrolyte membrane are schematically depicted in Fig. 3, which summarizes the dissolution of PVA in an acidic solution, incorporation of glycerol as a plasticizer, and subsequent addition of CQDs and CNTs prior to casting into membrane films. Polyvinyl Alcohol (PVA) was precisely measured to a quantity of 2 g. Following the preparation of all necessary components, a beaker was filled with 100 mL of distilled water, which was then stirred and heated with a magnetic stirrer set to 100 rpm for 5 min. Subsequently, 2 mL of hydrochloric acid (HCl) was introduced into the aqueous solution to facilitate the decomposition of the matrix. The requisite quantity of polyvinyl alcohol (PVA) was incorporated into the solution, succeeded by the addition of 1 mL of glycerol, which served as a plasticizing agent to augment the membrane's pliability. The solution was agitated incessantly for a duration of 60 min at a rotational speed of 150 revolutions per min until homogeneity was achieved. This investigation encompassed the fabrication of the electrolyte membrane in three distinct formulations: (1) a foundational solution comprising polyvinyl alcohol (PVA), hydrochloric acid (HCl), and glycerol; (2) a foundational solution supplemented with an additional 5 mL of Carbon

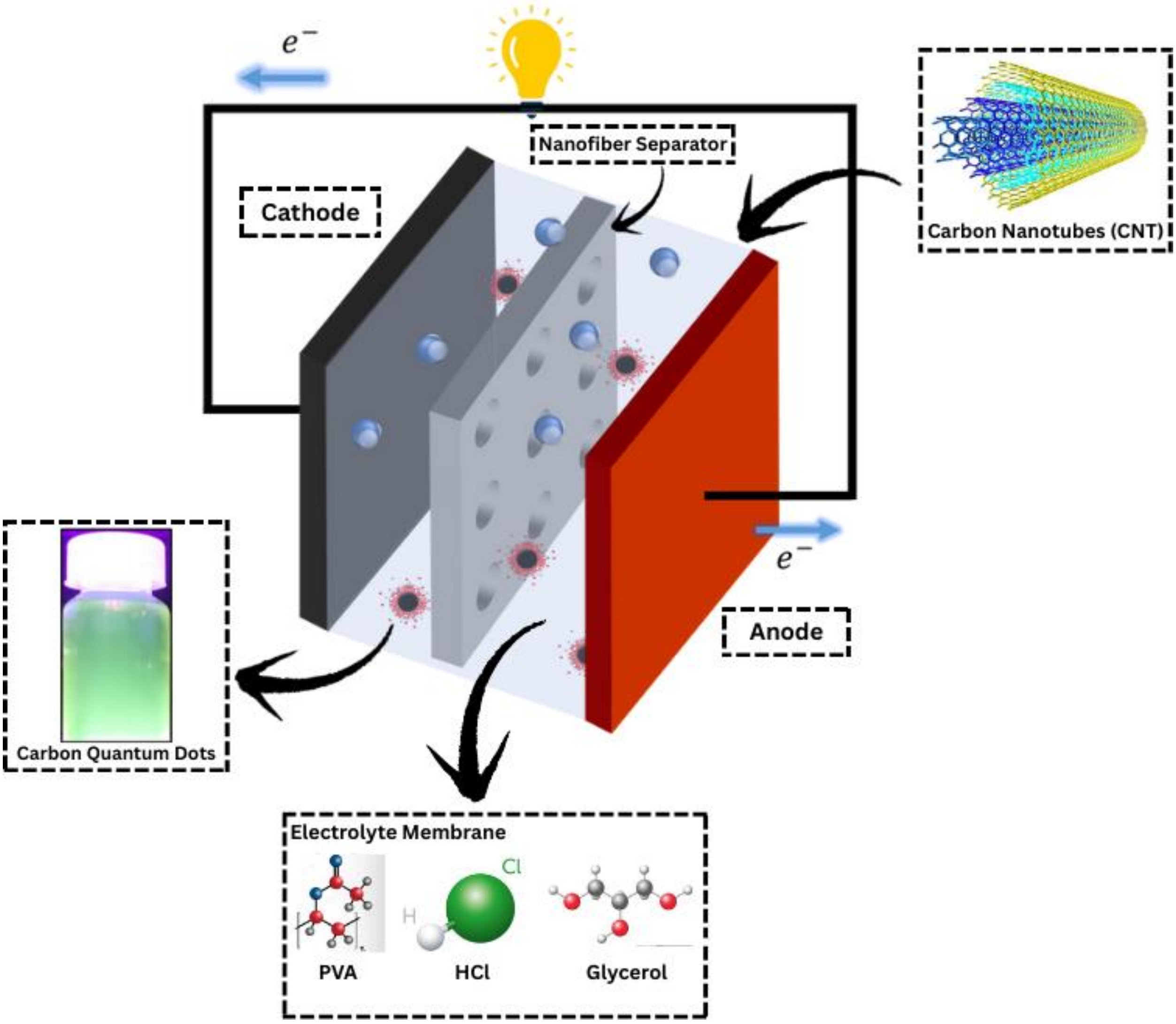

Fig. 3. Fabrication of gel electrolyte membrane

Quantum Dots (CQDs); and (3) a foundational solution containing 5 mL of CQDs 0.05 g of Carbon Nanotubes (CNT). Each formulation was carefully crafted to evaluate how the added materials affect the structural and performance properties of the resulting electrolyte membrane. In the second variation, 5 mL of CQDs solution was incrementally added to the base solution while stirring until complete integration was achieved. In the third variation, 0.05 g of CNTs were introduced into the base solution mixture, which already contained CQDs, and stirred until a homogeneous mixture was obtained. Once the mixing process was complete, the resultant solution from each variant was subsequently deposited into a Petri dish with a diameter of 10 cm for the purpose of desiccation. Initially, fifty percent of the solution was deposited into the dish, subsequently succeeded by the positioning of the pre-fabricated nanofiber layer atop. The residual solution was subsequently incorporated to guarantee that the nanofiber surface was comprehensively enveloped. The resultant electrolyte membrane was allowed to undergo desiccation at ambient temperature for a duration of 72 h [43].

2.5. Characterization

The Fourier Transform-Infrared (FT-IR) spectrum is utilized to detect molecular vibrations, examine compounds, and assess absorption intensity at particular wavelengths. FTIR analyses were meticulously performed utilizing a sophisticated PerkinElmer Frontier C90704 Spectrum IR Instrument, which operates on the advanced Version 10.6.1 software, ensuring precise and accurate spectral data acquisition for comprehensive analysis [44]. X-ray diffraction (XRD) analysis was meticulously executed utilizing a PANalytical X'Pert PRO diffractometer, which is equipped with a PW3050/60 goniometer that operates on the principle of Cu Kα radiation, characterized by a wavelength of $\lambda = 1.5406$ Å, and it was calibrated to function at a voltage of 40 kV in conjunction with a current of 30 mA, while encompassing an extensive scan range that spans from 5° to 100° in terms of 2θ, with a precise step size established at 0.02°. Electrochemical Impedance Spectroscopy, commonly referred to by the abbreviation EIS, was meticulously carried out utilizing a sophisticated potentiostat device, which enabled precise measurements over an extensive frequency spectrum that varied from 100,000 hertz down to a remarkably low limit of 0.01 hertz, thereby facilitating a comprehensive analysis of the electrochemical characteristics of the system under investigation. The evaluation of the ionic conductivity was meticulously conducted through a comprehensive analysis of the impedance test outcomes, which were subsequently utilized to perform calculations in accordance with the widely accepted and traditionally employed ionic conductivity equation that is recognized in the field [45].

3. Results and Discussion

3.1. Fourier Transform Infrared (FTIR)

Fig. 4 illustrates the FTIR spectra for three distinct sample compositions: PVA/HCl/Glycerol, PVA/HCl/Glycerol/CQDs, and PVA/HCl/Glycerol/CQDs/CNTs. Each spectrum exhibits characteristic absorption peaks that signify the presence of major functional groups within the composite polymer membrane structure. The broad absorption peak at ~3291 cm^{-1} is attributed to the stretching vibrations of hydroxyl (–OH) groups, originating from PVA and glycerol, the primary components [46]. Upon the incorporation of CQDs and CNTs, a slight decrease in absorption intensity in this region is noted, suggesting hydrogen interactions between the –OH groups and the surface groups of both CQDs and CNTs. This observation indicates enhanced intermolecular interactions within the composite polymer network structure due to the addition of nanoparticles [47]. The absorption peak near 2940 cm^{-1} signifies the stretching vibrations of aliphatic C–H groups found in the PVA polymer's backbone [46]. The persistence and stability of this peak across all variations indicate that the polymer backbone remains intact despite modifications to the surface structure. Additionally, the peak at ~1650 cm^{-1} corresponds to the stretching vibrations of carbonyl (C=O) groups. The intensity of this peak progressively increases with the addition of CQDs and CNTs, indicating the contribution of carbonyl groups from surface oxygen on the CQDs as well as functional oxygen groups from the modified CNT surface [48]. This increase confirms the successful integration of carbon nanoparticles into the PVA-glycerol matrix. The sharp peak at ~1050 cm^{-1} is attributed to the C–O stretching of alcohol groups, predominantly originating from the PVA and glycerol structures [49]. The addition of CQDs and CNTs also results in a slight shift and increase in this region, indicating an interaction between the C–O groups and the nanoparticle surface [50]. Overall, the changes in FTIR intensity and peak shifts across the three compositions demonstrate that the addition of CQDs and CNTs not only modifies the local chemical structure but also enhances the interactions between functional groups within the system. This has the potential to improve mechanical stability, hydrogen bonding capacity, and ionic conductivity, rendering the PVA/HCl/Glycerol/CQDs/CNT composition a promising candidate for efficient polymer electrolyte membrane applications [51].

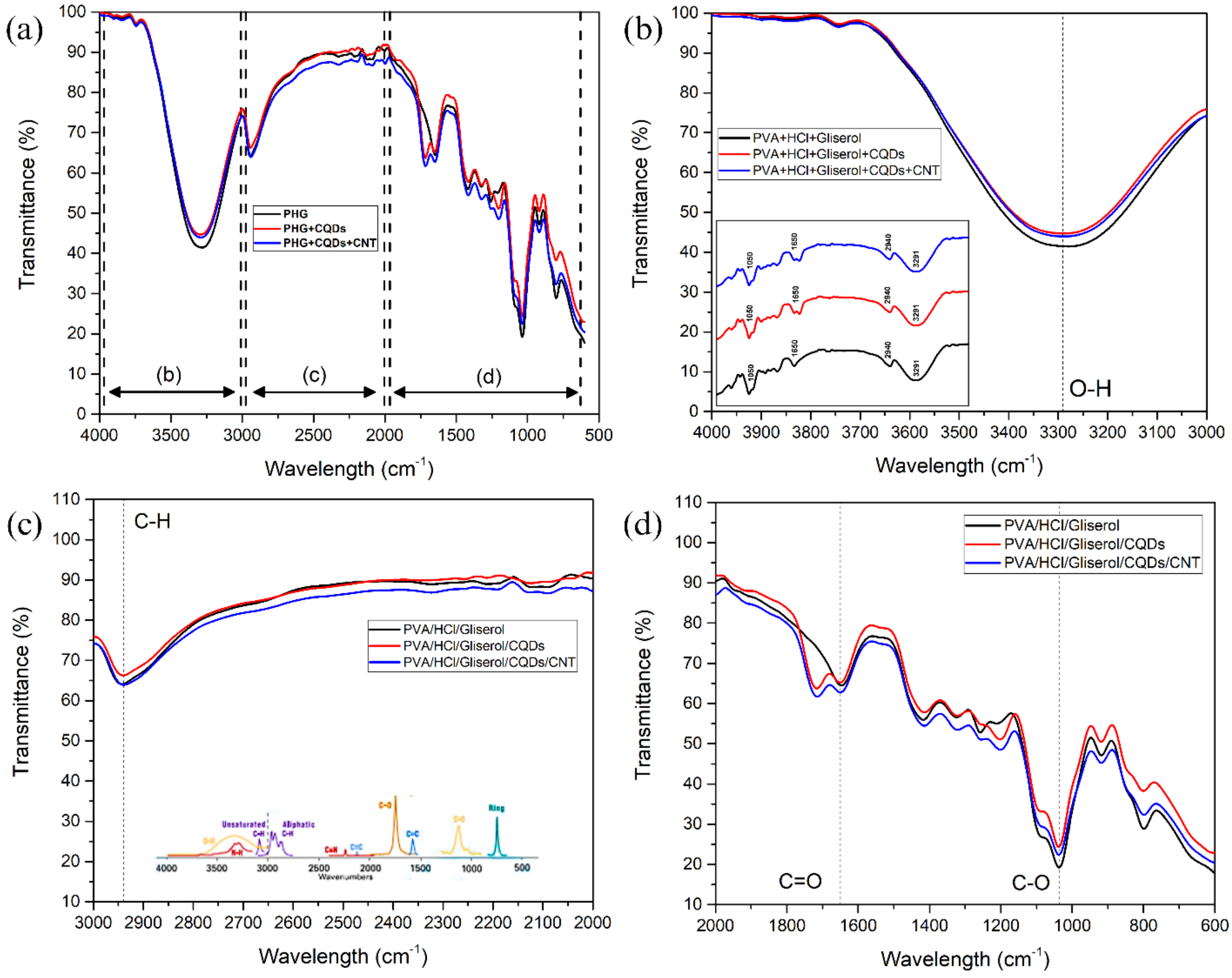

Fig. 4. FTIR spectrum of 3 variations of PVA/HCl/Glycerol electrolyte membrane at wavelengths (a) 4000-500 cm^{-1}, (b) 4000-3000 cm^{-1}, (c) 3000-2000 cm^{-1} and (d) 2000-600 cm^{-1}

The FTIR spectra also emphasized specific peak behaviors that confirmed enhanced intermolecular interactions. The reduction in the intensity of the O–H stretching vibration (~3291 cm^{-1}) signifies the enhancement of hydrogen bonding interactions between the hydroxyl moieties of polyvinyl alcohol (PVA)/glycerol and the surface functional groups of carbon quantum dots (CQDs)/carbon nanotubes (CNTs). The persistence of the C–H stretching at ~2940 cm^{-1} demonstrates that the polymer backbone remained stable despite nanoparticle incorporation. Meanwhile, the increase in the C=O stretching at ~1650 cm^{-1} reflects the contribution of carbonyl groups from CQDs/CNTs and their integration into the matrix. Finally, the shift and enhancement of the C–O stretching near ~1050 cm^{-1} suggest stronger interactions between the ether/alcohol groups and the nanoparticle surfaces. Collectively, the reduction, persistence, and enhancement of these peaks provide clear evidence of improved intermolecular interactions within the electrolyte membrane.

3.2. X-ray Diffraction (XRD)

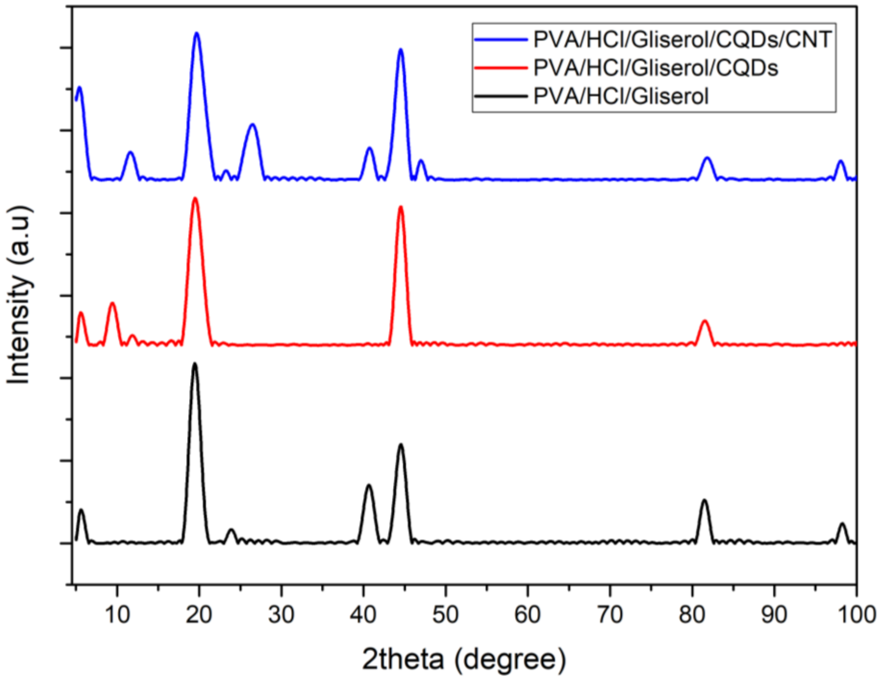

Fig. 5. XRD Chart of 3 variations of PVA/HCl/Glycerol electrolyte membrane

The X-ray diffraction patterns, which serve as crucial analytical representations of the structural characteristics inherent in various membrane samples, are depicted in Fig. 5 at a multitude of angles of incidence, thereby providing a comprehensive overview of the diffraction behavior observed in these specific materials under varying experimental conditions. These patterns illustrate the impact of incorporating additives such as Carbon Quantum Dots (CQDs) and Carbon Nanotubes (CNTs) on the intensity and morphology of the diffraction peaks, which are directly associated with alterations in crystallite size. Calculations employing the Scherrer equation [52,53], determined a crystallite size of 11.27 nm for the PVA/HCl/Glycerol membrane.

In contrast, the crystallite sizes for PVA/HCl/Glycerol/CQDs and PVA/HCl/Glycerol/CQDs/CNTs were found to be 9.65 nm and 8.29 nm, respectively. The reduction in crystallite size for both variants indicates a disruption in the crystalline structure's regularity due to the introduction of nanomaterials [54]. Specifically, the integration of CQDs into the PVA matrix inhibited crystallite growth, as evidenced by a reduction in crystallite size of approximately 1.6 nm [49]. This effect was further amplified by the addition of CNTs, which decreased the crystallite size to 8.29 nm. This reduction suggests that the presence of CNTs within the membrane structure enhances the amorphous characteristics and disrupts the molecular orientation necessary for crystal growth [55]. Overall, the progressive decrease in crystallite size from the baseline sample to the CNT-containing sample indicates that the incorporation of CQDs and CNTs effectively modifies the membrane's internal structure, potentially influencing the structural stability and ionic conductivity of the material.

3.3. Electrochemical Impedance Spectroscopy (EIS)

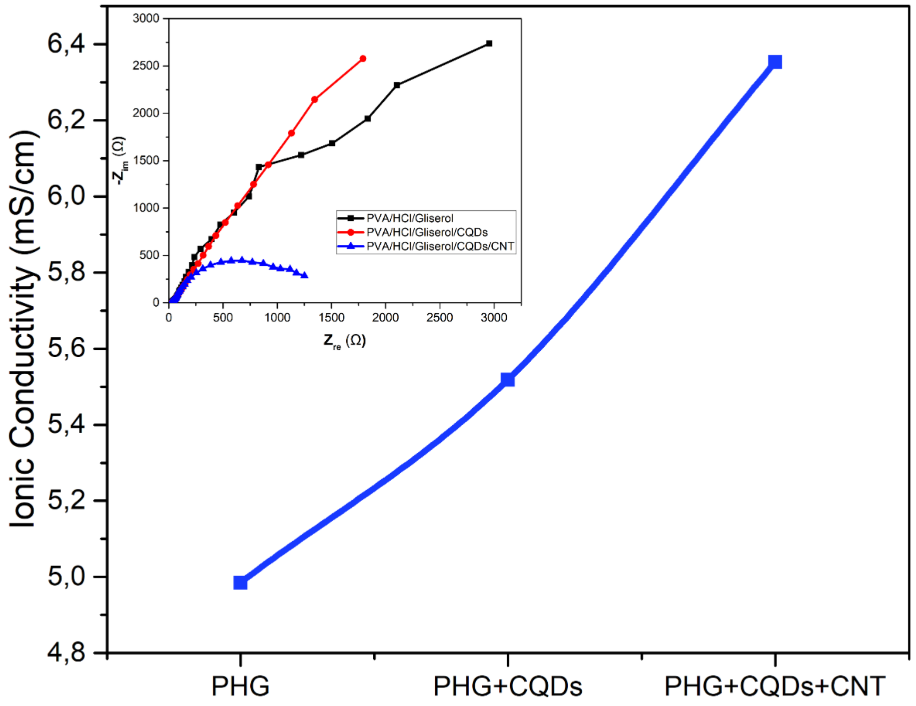

Fig. 6. Ionic Conductivity and Nyquist Plot of 3 Variations of PVA/HCl/Glycerol Electrolyte Membrane

Fig. 6 presents the electrode impedance analysis of three variations of electrolyte membranes: PHG (PVA/HCl/Glycerol), PHG + CQDs, and PHG + CQDs + CNTs. The Nyquist plot indicates that the PHG variation exhibits the highest impedance value, followed by PHG + CQDs, while PHG + CQDs + CNTs demonstrates the lowest impedance. The reduction in impedance value is inversely proportional to the increase in ionic conductivity, as depicted in Fig. 4. The PHG membrane recorded a conductivity of approximately 4.98501 mS/cm, which increased to 5.51837 mS/cm with the incorporation of CQDs, and further reached 6.35292 mS/cm upon the addition of CNTs. A lower impedance value corresponds to reduced ionic resistance in the electrolyte, facilitating faster and more efficient ion transfer [56]. This results in enhanced ionic conductivity due to the optimization of the ion migration pathway [57]. The incorporation of CQDs derived from rice husk charcoal enhances the internal structure of the membrane, thereby expanding the conductive pathway for ions [47]. The integration of CNTs further establishes a one-dimensional network that augments charge transport, both ionically and electronically [58]. This inverse linear relationship between impedance and conductivity suggests that the combination of CQDs and CNT additives not only reduces the internal resistance of the membrane but also significantly enhances the efficiency of the aluminium–air battery electrolyte.

4. Conclusions

This study focuses on enhancing the ionic conductivity, physical properties, and overall the enhancement of the operational efficiency and overall performance characteristics of aluminium–air battery electrolyte membranes can be significantly achieved through the innovative integration of carbon quantum dots (CQDs) that are meticulously derived from the pyrolysis of rice husk charcoal, in conjunction with the utilization of carbon nanotubes (CNTs), which are renowned for their remarkable electrical conductivity and mechanical strength. Three electrolyte membrane variations were prepared: a base solution of PVA/HCl/glycerol, a base solution with CQDs, and a base solution with both CQDs and CNTs. FTIR analysis showed that the addition of CQDs and CNTs enhanced the intermolecular interactions within the composite polymer network. The XRD patterns revealed a progressive decrease in the crystallite size with the incorporation of CQDs and CNTs, indicating a disruption in the regularity of the crystalline structure. Electrochemical impedance spectroscopy demonstrated that the addition of CQDs and CNTs significantly reduced the impedance value and increased the ionic conductivity, with the PHG + CQDs + CNTs membrane exhibiting the highest conductivity at 6.35292 mS/cm.

The nanofiber architecture can support ion transport, increase electrolyte uptake, and contribute to safety and thermal stability, as reported in previous studies. This study highlights the potential of using renewable resources, such as rice husk charcoal, to develop cost-effective and environmentally sustainable solutions for high-performance aluminium–air batteries. Nevertheless, this study did not include a direct evaluation of the mechanical strength of the membranes, which remains an important parameter for long-term stability. Therefore, future studies should focus on tensile and elongation testing to quantitatively assess the mechanical properties of the developed membranes. Subsequent and more comprehensive investigations are necessitated to thoroughly tackle and resolve the multifaceted challenges associated with the process of scaling up aluminium–air battery systems; these challenges encompass critical aspects such as the stability of the electrodes over prolonged use, the long-term durability and performance of the electrolyte under various operating conditions, and the effective integration of these systems into practical and commercially viable device architectures that can be utilized in real-world applications. Addressing these obstacles is pivotal for the progression of aluminium–air technology towards practical implementations in extensive energy storage solutions and mobile power systems.

Data availability statement

Data will be made available on request.

CRediT authorship contribution statement

Firman Ridwan: Validation, Methodology, Conceptualization. **Muhammad Ammar Zakky:** Writing – original draft, Investigation, Data curation, Visualization. **Dean Bilalwa Agusto:** Software. **Wismalqi:** Formal analysis. **Gusriwandi:** Supervision.

Declaration of Competing Interest

The authors declare that they have no known financial conflicts of interest or personal relationships that could have appeared to influence the work reported in this paper.

Acknowledgement

This research is funded by: ANDALAS UNIVERSITY, in accordance with the Research Contract, Batch I Undergraduate Thesis Research Scheme, Number: 230/UN16.19/PT.01.03/PSS/2025, Fiscal Year 2025.

References

[1] Deirmentzoglou GA, Anastasopoulou EE, Sklias P. International economic relations and energy security in the European Union: a systematic literature review. Int J Sustain Energy 2024;43:1–13. https://doi.org/10.1080/14786451.2024.2385682.

[2] Siow JH, Bilad MR, Caesarendra W, Leam JJ, Bustam MA. Progress in Development of Nanostructured Manganese Oxide 2021:1–16. https://doi.org/10.3390/en14196385

[3] Wang ZQ, Chen HM, Liu XD, Song LY, Zhang BS, Yang YG, *et al.* Amorphous K-Buserite Microspheres for High-Performance Aqueous Zn-Ion Batteries and Hybrid Supercapacitors. Adv Sci 2023;10:1–15. https://doi.org/10.1002/advs.202207329.

[4] Nugroho AP, Hawari NH, Prakoso B, Refino AD, Yulianto N, Iskandar F, *et al.* Vertically aligned n-type silicon nanowire array as a free-standing anode for lithium-ion batteries. Nanomaterials 2021;11. https://doi.org/10.3390/nano11113137.

[5] Ma D, Li J, Li H, Yuan D, Ji Z, Manawan M, *et al.* Progress of Advanced Cathode Materials of Rechargeable Aluminum-Ion Batteries. Energy Mater Adv 2024;5. https://doi.org/10.34133/energymatadv.0088.

[6] Sumboja A, Prakoso B, Ma Y, Irwan FR, Hutani JJ, Mulyadewi A, *et al.* FeCo Nanoparticle-Loaded Nutshell-Derived Porous Carbon as Sustainable Catalyst in Al-Air Batteries. Energy Mater Adv 2021;2021. https://doi.org/10.34133/2021/7386210.

[7] Jumari A, Yudha CS, Widiyandari H, Lestari AP, Rosada RA, Santosa SP, *et al.* Sio2/c composite as a high capacity anode material of lini0.8co0.15al0.05o2 battery derived from coal combustion fly ash. Appl Sci 2020;10:1–13. https://doi.org/10.3390/app10238428.

[8] Riza Putra B, Tshwenya L, Buckingham MA, Chen J, Jeremiah Aoki K, Mathwig K, *et al.*

Microscale Ionic Diodes: An Overview. Electroanalysis 2021;33:1398–418. https://doi.org/10.1002/elan.202060614.

[9] Ndruru STCL, Pramono E, Wahyuningrum D, Bundjali B, Arcana IM. Preparation and characterization of biopolymer blend electrolyte membranes based on derived celluloses for lithium-ion batteries separator. Bull Mater Sci 2021;44. https://doi.org/10.1007/s12034-021-02369-7.

[10] Handayani M, Hendrik, Abbas A, Anshori I, Mulyawan R, Satriawan A, *et al.* Development of graphene and graphene quantum dots toward biomedical engineering applications: A review. Nanotechnol Rev 2023;12:1–42. https://doi.org/10.1515/ntrev-2023-0168.

[11] Saafie N, Sambudi NS, Wirzal MDH, Sufian S. Effect of Hydrothermal Conditions on Kenaf-Based Carbon Quantum Dots Properties and Photocatalytic Degradation. Separations 2023;10. https://doi.org/10.3390/separations10020137.

[12] Steven S, Restiawaty E, Pasymi P, Bindar Y. Influences of pretreatment, extraction variables, and post treatment on bench-scale rice husk black ash (RHBA) processing to bio-silica. Asia-Pacific J Chem Eng 2021;16:1–10. https://doi.org/10.1002/apj.2694.

[13] Zhang M, Ning G, Xiao Z. Binder-Assisted Dispersion of Agglomerated Carbon Nanotubes for Efficiently Establishing Conductive Networks in Cathodes of Li-Ion Batteries. Energy Technol 2020;8:1–7. https://doi.org/10.1002/ente.202000589.

[14] Wang Y, Tang L, Li Y, Li Q, Bai B. Preparation of modified multi-walled carbon nanotubes as a reinforcement for epoxy shape-memory polymer composites. Polym Adv Technol 2021;32:67–75. https://doi.org/10.1002/pat.5061.

[15] Zulfajri M, Sudewi S, Ismulyati S, Rasool A, Adlim M, Huang GG. Carbon dot/polymer composites with various precursors and their sensing applications: A review. Coatings 2021;11. https://doi.org/10.3390/coatings11091100.

[16] Ji S, Mou Y, Liu H, Lu X, Zhang Y, Guo C, *et al.* Manipulating the Electronic Properties of an Fe Single Atom Catalyst via Secondary Coordination Sphere Engineering to Provide Enhanced Oxygen Electrocatalytic Activity in Zinc-Air Batteries. Adv Mater 2024;36:2410121. https://doi.org/10.1002/ADMA.202410121.

[17] Lan F, Zhao H, Jiang Y, Jin C, Zhao G, Li L. A thermomechanically stable nanofiber separator with multiscale MOF networks towards high-efficiency ion transport. J Mater Chem A 2025;13:7357–70. https://doi.org/10.1039/d4ta07790c.

[18] Yang W, Liu Y, Hu X, Yao J, Chen Z, Hao M, *et al.* Multilayer nanofiber composite separator for lithium-ion batteries with high safety. Polymers (Basel) 2019;11. https://doi.org/10.3390/polym11101671.

[19] Liu M, Zhang P, Qu Z, Yan Y, Lai C, Liu T, *et al.* Conductive carbon nanofiber interpenetrated graphene architecture for ultra-stable sodium ion battery. Nat Commun 2019;10. https://doi.org/10.1038/s41467-019-11925-z.

[20] Zheng M, Chi Y, Hu Q, Tang H, Jiang X, Zhang L, *et al.* Carbon nanotube-based materials for lithium-sulfur batteries. J Mater Chem A 2019;7:17204–41. https://doi.org/10.1039/c9ta05347f.

[21] Abdul Razzaq A, Yao Y, Shah R, Qi P, Miao L, Chen M, *et al.* High-performance lithium sulfur batteries enabled by a synergy between sulfur and carbon nanotubes. Energy Storage Mater 2019;16:194–202. https://doi.org/10.1016/j.ensm.2018.05.006.

[22] Palanisamy S, Shyma AP, Srinivasan S, Venkatachalam R. Novel modified nano-activated carbon and its influence on the metal–O 2 battery system. J Energy Storage 2019;22:283–94. https://doi.org/10.1016/j.est.2019.02.006.

[23] Yang H, Li X, Wang Y, Gao L, Li J, Zhang D, *et al.* Excellent performance of aluminium anode based on dithiothreitol additives for alkaline aluminium/air batteries. J Power Sources 2020;452:227785. https://doi.org/10.1016/J.JPOWSOUR.2020.227785.

[24] Mori R. Recent Developments for Aluminum–Air Batteries. Electrochem Energy Rev 2020;3:344–69. https://doi.org/10.1007/s41918-020-00065-4.

[25] Hu Y, Chen W, Lei T, Jiao Y, Wang H, Wang X, *et al.* Graphene quantum dots as the

nucleation sites and interfacial regulator to suppress lithium dendrites for high-loading lithium-sulfur battery. Nano Energy 2020;68:104373. https://doi.org/10.1016/J.NANOEN.2019.104373.

[26] Zhu Y, Li J, Yun X, Zhao G, Ge P, Zou G, *et al.* Graphitic Carbon Quantum Dots Modified Nickel Cobalt Sulfide as Cathode Materials for Alkaline Aqueous Batteries. Nano-Micro Lett 2020;12:1–18. https://doi.org/10.1007/S40820-019-0355-0.

[27] Zhou Y, Shu H, Zhou Y, Sun T, Han M, Chen Y, *et al.* Flower-like Bi4Ti3O12/Carbon nanotubes as reservoir and promoter of polysulfide for lithium sulfur battery. J Power Sources 2020;453:227896. https://doi.org/10.1016/J.JPOWSOUR.2020.227896.

[28] Sun M, Xu Z, Liu K, Yang H, Yang T, Jin C, *et al.* Construction of rice husk-derived SiOx nanoparticles encapsulated with graphene aerogel hybrid for high-performance lithium ion batteries. Electrochim Acta 2022;422:140572. https://doi.org/10.1016/J.ELECTACTA.2022.140572.

[29] Sun X, Liu W, Xu D, Shi L, Qi P, Xiong Y, *et al.* The influence of the characteristics of rice husk-based activated carbon on the performance of lead-carbon batteries and its potential mechanisms. Electrochim Acta 2022;403:139688. https://doi.org/10.1016/J.ELECTACTA.2021.139688.

[30] Kumar S, Goswami M, Singh N, Sathish N, Reddy M V., Kumar S. Exploring carbon quantum dots as an aqueous electrolyte for energy storage devices. J Energy Storage 2022;55:105522. https://doi.org/10.1016/J.EST.2022.105522.

[31] Liu S, Ban J, Shi H, Wu Z, Shao G, Cao G, *et al.* Near solution-level conductivity of polyvinyl alcohol based electrolyte and the application for fully compliant Al-air battery. Chem Eng J 2022;431:134283. https://doi.org/10.1016/J.CEJ.2021.134283.

[32] Luo W, Chen W, Quan H, Zhang ZX, Zeng Y, Wang Y, *et al.* Strongly coupled carbon quantum dots/NiCo-LDHs nanosheets on carbon cloth as electrode for high performance flexible supercapacitors. Appl Surf Sci 2022;591:153161. https://doi.org/10.1016/J.APSUSC.2022.153161.

[33] Lu Z, Hu Z, Xiao L, Xie Y, Li N, Xi L, *et al.* Battery-type Ni-Co-Se hollow microspheres cathode materials enabled by bifunctional N-doped carbon quantum dots with ultrafast electrochemical kinetics for hybrid supercapacitors. Chem Eng J 2022;450:138347. https://doi.org/10.1016/J.CEJ.2022.138347.

[34] Wang R, Liu J, Xie J, Cai Z, Yu Y, Zhang Z, *et al.* Hollow nanocage with skeleton Ni-Fe sulfides modified by N-doped carbon quantum dots for enhancing mass transfer for oxygen electrocatalysis in zinc-air battery. Appl Catal B Environ 2023;324:122230. https://doi.org/10.1016/J.APCATB.2022.122230.

[35] Shaker M, Shahalizade T, Mumtaz A, Hemmati Saznaghi M, Javanmardi S, Gaho MA, *et al.* A review on the role of graphene quantum dots and carbon quantum dots in secondary-ion battery electrodes. FlatChem 2023;40:100516. https://doi.org/10.1016/J.FLATC.2023.100516.

[36] Pallavolu MR, Prabhu S, Nallapureddy RR, Kumar AS, Banerjee AN, Joo SW. Bio-derived graphitic carbon quantum dot encapsulated S- and N-doped graphene sheets with unusual battery-type behavior for high-performance supercapacitor. Carbon N Y 2023;202:93–102. https://doi.org/10.1016/J.CARBON.2022.10.077.

[37] Patwari MAU, Hossain A, Maroof I, Mahmud MF. An Innovative Approach to Assess the Potentiality of Using Activated Carbon and Rice Husk Ash in AIuminum-Air Battery. Malaysian J Compos Sci Manuf 2024;13:55–67. https://doi.org/10.37934/mjcsm.13.1.5567

[38] Hoang AT, Pandey A, Huang Z, Luque R, Ng KH, Papadopoulos AM, *et al.* Catalyst-Based Synthesis of 2,5-Dimethylfuran from Carbohydrates as a Sustainable Biofuel Production Route. ACS Sustain Chem Eng 2022;10:3079–115. https://doi.org/10.1021/acssuschemeng.1c06363.

[39] Suman, Rani G, Ahlawat R, Kumar H. Green source-based carbon quantum dots, composites, and key factors for high-performance of supercapacitors. J Power Sources

2024;617:235170. https://doi.org/10.1016/j.jpowsour.2024.235170.

[40] Xu L, Li Y, Gao S, Niu Y, Liu H, *et al.* Preparation and Properties of Cyanobacteria-Based Carbon Quantum Dots / Polyvinyl Alcohol / Nanocellulose Composite. Polymers 2020;12:1–12. https://doi.org/10.3390/polym12051143

[41] Rezaei F, Gorbanev Y, Chys M, Nikiforov A, Van Hulle SWH, Cos P, *et al.* Investigation of plasma-induced chemistry in organic solutions for enhanced electrospun PLA nanofibers. Plasma Process Polym 2018;15:1–18. https://doi.org/10.1002/ppap.201700226.

[42] Wang D, Li X, Zou Z, Wang B, Yao D, Han Y, *et al.* Ultrasonic assisted electrospinning preparation the polylactic acid loading with perillaldehyde biopolymer film with excellent solvent resistance, water-oxygen barrierstability and preservation effect. Lwt 2024;211:116859. https://doi.org/10.1016/j.lwt.2024.116859.

[43] Ridwan F, Husin MA, Febriyan N. Synthesis of a Gel Electrolyte Membrane Based on PVA/KCl/Glycerol Doped with CQDs for Aluminum Ion Battery Applications. Rev Des Compos Des Mater Av 2025;35:87–95. https://doi.org/10.18280/rcma.350111.

[44] Junoh H, Jaafar J, Nor NAM, Awang N, Norddin MNAM, Ismail AF, *et al.* Fabrication of nanocomposite membrane via combined electrospinning and casting technique for direct methanol fuel cell. J Membr Sci Res 2018;4:146–57. https://doi.org/10.22079/JMSR.2017.68712.1149.

[45] Tsai HW, Tampubolon NF, Wu T, Wu MY, Lin YW. Characterization of carbon dots from fructus gardeniae (Zhi-zi) and gardenia charcoal (black Zhi-zi) via microwave-assisted extraction. J Food Drug Anal 2024;32:371–81. https://doi.org/10.38212/2224-6614.3513.

[46] Sunaryono S, Rachmawati A, Yogihati CI, Susanto H, Taufiq A, Mufti N. The effect of Ag nanoparticles in Ag/polyvinyl alcohol nanofiber composites. Polym Bull 2022;79:555–68. https://doi.org/10.1007/s00289-020-03528-2.

[47] Falara PP, Ibrahim I, Zourou A, Sygellou L, Sanchez DE, Romanos GE, *et al.* Bi-functional photocatalytic heterostructures combining titania thin films with carbon quantum dots (C-QDs/TiO2) for effective elimination of water pollutants. Environ Sci Pollut Res 2023;30:124976–91. https://doi.org/10.1007/s11356-023-27285-7.

[48] Nazar M, Hasan M, Wirjosentono B, Gani BA, Nada CE. Microwave Synthesis of Carbon Quantum Dots from Arabica Coffee Ground for Fluorescence Detection of Fe3+, Pb2+, and Cr3+. ACS Omega 2024;9:20571–81. https://doi.org/10.1021/acsomega.4c02254.

[49] Waresindo WX, Luthfianti HR, Edikresnha D, Suciati T, Noor FA, Khairurrijal K. A freeze-thaw PVA hydrogel loaded with guava leaf extract: physical and antibacterial properties. RSC Adv 2021;11:30156–71. https://doi.org/10.1039/d1ra04092h.

[50] Setianto S, Men LK, Bahtiar A, Panatarani C, Joni IM. Carbon quantum dots with honeycomb structure: a novel synthesis approach utilizing cigarette smoke precursors. Sci Rep 2024;14:1–8. https://doi.org/10.1038/s41598-024-52106-3.

[51] Mahmoud A, Fahmy A, Naser A, Saied MA. Novel sulfonated poly (vinyl alcohol)/carboxy methyl cellulose/acrylamide-based hybrid polyelectrolyte membranes. Sci Rep 2022;12:1–15. https://doi.org/10.1038/S41598-022-26489-0.

[52] Supiyani, Agusnar H, Sugita P, Nainggolan I. Preparation sodium silicate from rice husk to synthesize silica nanoparticles by sol-gel method for adsorption water in analysis of methamphetamine. South African J Chem Eng 2022;40:80–6. https://doi.org/10.1016/j.sajce.2022.02.001.

[53] Daulay A, Andriayani, Marpongahtun, Gea S. Synthesis Si nanoparticles from rice husk as material active electrode on secondary cell battery with X-Ray diffraction analysis. South African J Chem Eng 2022;42:32–41. https://doi.org/10.1016/j.sajce.2022.07.004.

[54] Sunaryono S, Hidayat MF, Mufti N, Soontaranon S, Taufiq A. The effect of Mn doping on nano structure and magnetic properties of MnxFe3-xO4-PEG/PVP/PVA based ferrogel. J Polym Res 2020;27. https://doi.org/10.1007/s10965-020-02065-w.

[55] Xiang D, Shui T, Qiao H, Tan W, Harkin-Jones E, Zhang J, *et al.* Enhanced interfacial interaction, mechanical properties and thermal stability of basalt fiber/epoxy composites

with multi-scale reinforcements. Compos Interfaces 2023;30:1387–409. https://doi.org/10.1080/09276440.2023.2220500.

[56] Darmawan DA, Yulianti E, Sabrina Q, Ishida K, Sakti AW, Nakai H, *et al.* Fabrication of solid polymer electrolyte based on carboxymethyl cellulose complexed with lithium acetate salt as Lithium-ion battery separator. Polym Compos 2024;45:2032–49. https://doi.org/10.1002/PC.27902.

[57] Puspitasari DA, Patra J, Hernandha RFH, Chiang YS, Inoishi A, Chang BK, *et al.* Enhanced Electrochemical Performance of Ca-Doped Na3V2(PO4)2F3/C Cathode Materials for Sodium-Ion Batteries. ACS Appl Mater Interfaces 2024;16:496–506. https://doi.org/10.1021/acsami.3c12772.

[58] Wahyuni WT, Ta'alia SAH, Akbar AY, Elvira BR, Irkham N, Rahmawati I, *et al.* Electrochemical sensors based on the composite of reduced graphene oxide and a multiwalled carbon nanotube-modified glassy carbon electrode for simultaneous detection of hydroquinone, dopamine, and uric acid. RSC Adv 2024;38:27999–8016. https://doi.org/10.1039/D4RA05537C.